

The erosion of granular beds under the action of fluid shearing flows

Pascale Aussillous, Julien Chauchat^a, Malika Ouriemi^b,
Marc Médale, Mickaël Pailha^c, Yannick Peysson^b,
and Élisabeth Guazzelli

Aix-Marseille Université, CNRS, IUSTI

^a UJF – INPG, CNRS, LEGI

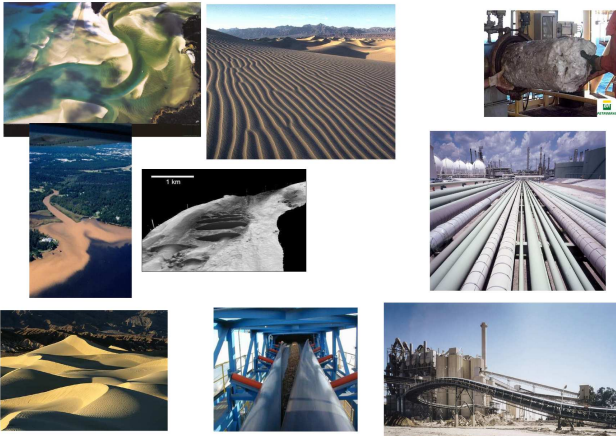
^b IFP Energies Nouvelles

^c Université de Savoie, CNRS, LOCIE

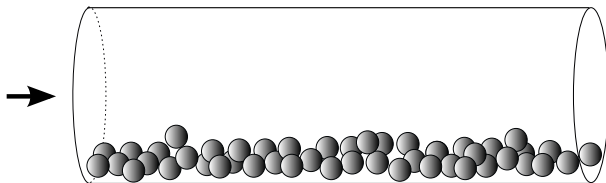
Fundings: IFP Energies Nouvelles, ANR Project Dunes

GEOFLO16 – Max Planck Institute in Dresden

Sediment transport and self-formed morphologies



Bed-load transport in pipe flows



What parameters characterize:

- 1 the incipient motion of the grains?
- 2 the rate of particle transport?
- 3 the formation of dunes?

- 1 Incipient motion
- 2 Bed-load transport: a two-phase approach
- 3 Inside the bed-load
- 4 Bed-load transport: a discrete approach
- 5 Dunes

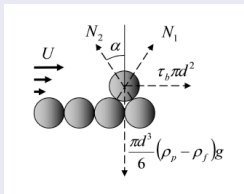
- 1 Incipient motion
- 2 Bed-load transport: a two-phase approach
- 3 Inside the bed-load
- 4 Bed-load transport: a discrete approach
- 5 Dunes

Incipient motion characterized by critical Shields number

Shields number: $\theta = \tau_b / (\rho_p - \rho_f)gd$

α ratio of the fluid force on the particle to the weight of the particle

Force balance on a grain



$$\tau_b \pi d^2 + (N_1 - N_2) \sin \alpha = 0$$

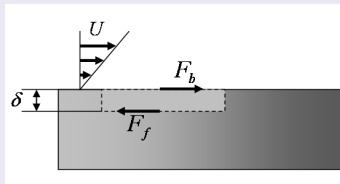
$$\frac{\pi}{6} d^3 (\rho_p - \rho_f) g - (N_1 + N_2) \cos \alpha = 0$$

At threshold, contact with first grain lost ($N_1 \equiv 0$)

$$\therefore \frac{\tau_b}{(\rho_p - \rho_f)gd} = \frac{1}{6} \tan \alpha$$

$$\rightarrow \theta^c \approx 0.1 \text{ (for } \alpha = 30^\circ \text{)}$$

Force balance on a grain layer



Shearing forces: $F_b = \tau_b dS$
 Coulomb friction: $F_f = \mu F_N$
 with normal force $F_N = dS \delta (\rho_p - \rho_f) g \phi$

At threshold, thickness of the mobile layer $\delta \equiv d$

$$\therefore \frac{\tau_b}{(\rho_p - \rho_f)gd} = \mu \phi$$

$$\rightarrow \theta^c \approx 0.3 \text{ (for } \mu = 0.5 \text{ and } \phi = 0.6 \text{)}$$

Shields curve

from Buffington 1999

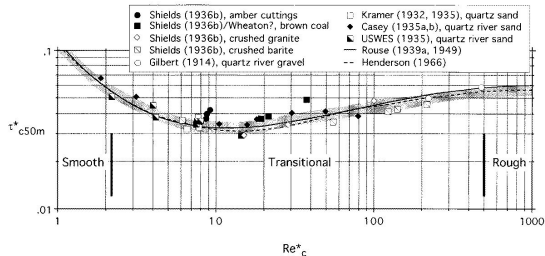


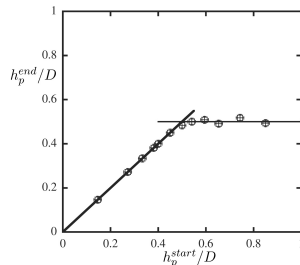
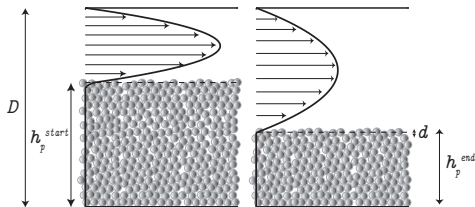
FIG. 4. τ_{*c}^{*50m} as Function of Re_c^{*c} , Redrafted from Shields (1936b). Shaded Band with Irregular Boundaries Is Data Envelope and Curve Fit as Defined by Shields. Solid and Dashed Lines Are Later Fits of These Data by Subsequent Authors. Note that Gilbert and USWES Values Are Actually for τ_{*cr}^{*50m} Which Differs from that of τ_{*c}^{*50m} Only for USWES

Large scatters due to:

- Bed packing conditions
- Polydispersity in size
- Multiple possible definition for the onset of grain motion
- Different definition of the shear stress

Threshold characterized through cessation of motion

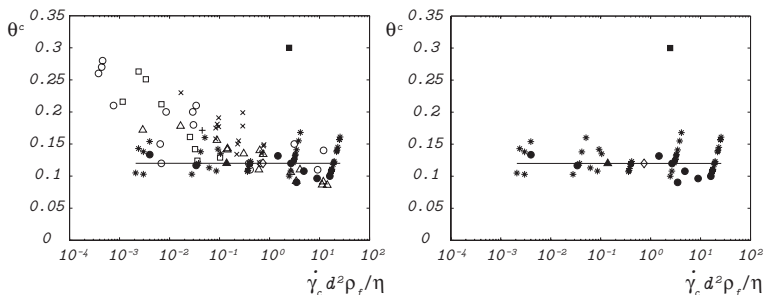
A granular bed submitted to a laminar flow in a pipe (test section not fed in with particles)



$$\theta^c = 0.12 \pm 0.03 \text{ in the range } 1.5 \cdot 10^{-5} \leq Re_p \leq 0.76$$

Ouriemi, Aussillous, Médale, Peysson, and Guazzelli PoF 2007

Shields curve in the laminar regime



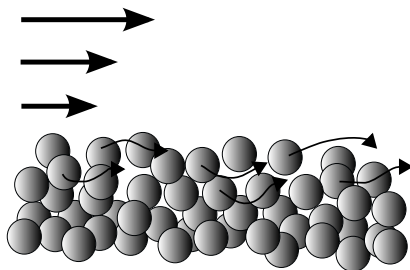
White 1940 (+), White 1970 (\square), Mantz 1977 (\times), Yalin *et al.* 1979 (\triangle), Pilotti *et al.* 2001 (\circ), Charru *et al.* 2004 (\blacktriangle), Loiseleux *et al.* 2005 (\bullet), Ouriemi *et al.* 2007 ($*$), Lobkovsky *et al.* 2008 (\blacksquare), Malverti *et al.* 2008 (\diamond)

Recent controlled experiments: $\theta^c \approx 0.12$ independent of Re

Direct numerical simulations of Derksen PoF 2011 and Kidanemariam and Uhlmann IJMF 2014 in line with experiments

- 1 Incipient motion
- 2 Bed-load transport: a two-phase approach**
- 3 Inside the bed-load
- 4 Bed-load transport: a discrete approach
- 5 Dunes

Bed-load transport



Typical findings: $q_p \propto \theta^n$

Einstein 1942, 1950, Bagnold 1956, Yalin 1963 ...

In laminar regime: $q_p \propto \theta^2$ near θ^c and $\propto \theta^3$ away from θ^c

Charru, Mouilleron, and Eiff 2004, 2009, Ouriemi, Aussillous, and Guazzelli 2009

Two-phase model of bed-load transport

Two-phase equations (see Jackson 1997, 2000)

- Continuity equations for the fluid and particle phases
- Momentum equations for the fluid and particle phases

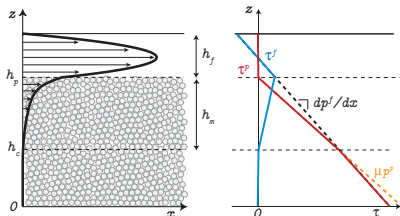
Closures (Ouriemi, Aussillous, and Guazzelli JFM 2009 Part 1)

- Particle-fluid interaction: **viscous Darcy drag**
- Newtonian rheology for the fluid phase: $\tau^f = \eta_e \dot{\gamma}$
- Frictional rheology (contact interactions) in the mobile granular layer: $\tau^p = \mu p^p$

Resulting equations for viscous shearing flows

- Brinkman equation for the fluid phase
→ **Darcy term dominant**
- Mixture equation (suspension balance)
→ **Exchange between stresses of the fluid and solid phases**
- Hydrostatic pressure
→ $p^p = \phi \Delta \rho g (h_p - z)$ **apparent weight of the solid phase**

Simple calculation for Coulomb friction and constant ϕ



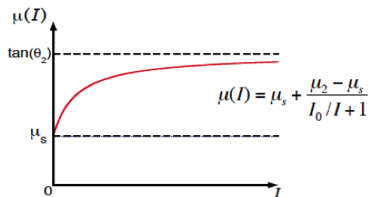
- μ and $\eta_e = \text{constant}$
- Darcy dominant \rightarrow no slip: $U \approx u^p \approx u^f$
- Mixture: $\tau^p(z) + \tau^f(z) = \tau^f(h_p) - \frac{\partial p^f}{\partial x}(h_p - z)$
 $\tau^f = \eta_e \frac{\partial U}{\partial z}$: $\equiv \tau^f(h_p)$ at h_p and goes to 0 at h_c
 $\tau^p = \mu p^p = \mu \phi \Delta \rho g (h_p - z)$:
 $\equiv 0$ at h_p and increases until can keep $\equiv \mu p^p$ (i.e. until h_c)

- Bed-load thickness: $\frac{h_m}{h_f} = \frac{\eta_e}{\eta} \left[1 - \sqrt{1 - \frac{\eta}{\eta_e} \frac{\partial p^f / \partial x}{\partial p^f / \partial x + \mu \phi \Delta \rho g}} \right]$
- Parabolic velocity profile: $u^p = u^f = U = \frac{\partial p^f / \partial x + \mu \phi \Delta \rho g}{\eta_e} \frac{(z - h_c)^2}{2}$

Relevant scalings

length scale = h_f , pressure scale = $\Delta \rho g h_f$, time scale = $\eta / \Delta \rho g h_f$
 control parameter = fluid flow rate q_f made dimensionless by $\Delta \rho g h_f^3 / \eta$

More sophisticated granular frictional rheology



Shear-dependent friction law:

$$\mu(I) = \mu_s + I(\mu_2 - \mu_s)/(I + I_0)$$

(GDR Midi 2004, da Cruz *et al.* 2005, Jop *et al.* 2006 ...)

Single dimensionless control parameter for hard spheres: dimensionless shear rate I

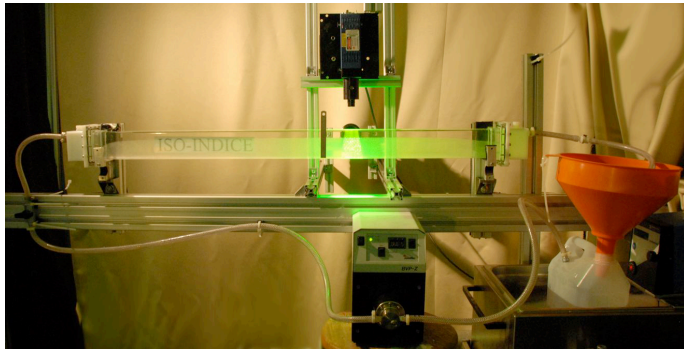
- Dry granular flows: inertial number
 $I = d\sqrt{\rho_p/p^p}\dot{\gamma}$
- Wet granular flows: viscous number
 $I_v = \eta\dot{\gamma}^p/p^p$ (Cassar *et al.* 2005)

Numerical implementation

- Nonlinear mixture equation through the constitutive laws for $\mu(I_v)$, $\phi(I_v)$, and $\eta_e(\phi)$ solved numerically using MATLAB
- Full three dimensional case: finite-element code + regularisation technique for frictional granular rheology (Chauchat and Médale *Comput. Methods Appl. Mech. Engrg.* 2010)

- 1 Incipient motion
- 2 Bed-load transport: a two-phase approach
- 3 Inside the bed-load**
- 4 Bed-load transport: a discrete approach
- 5 Dunes

Granular bed in a rectangular-tube flow

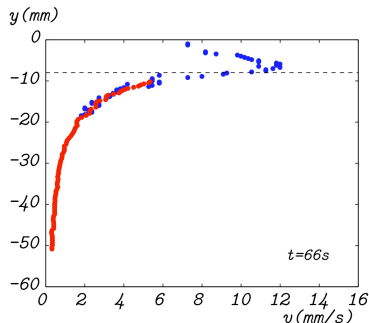
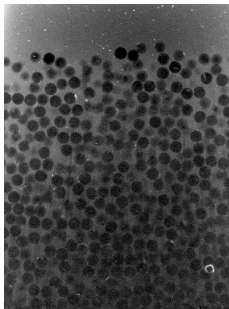


- Two index-matched combinations of fluids and particles (Borosilicate + mixture of Triton X-100 and water as well as PMMA + Triton X-100)
- Viscous laminar regime: Both θ and Re range from 0.2 to 1.2

Aussillous, Chauchat, Pailha, Médale, and Guazzelli JFM 2013
inspired by Goharzadeh *et al.* PoF 2005 and Lobkovsky *et al.* JFM 2008

Inside the mobile granular bed

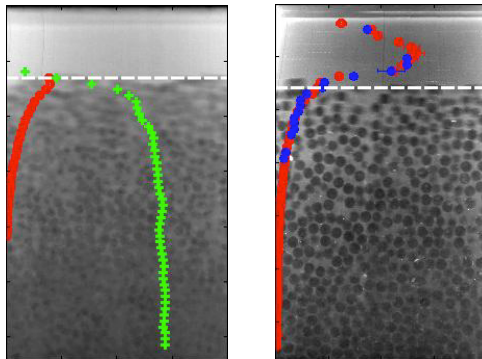
PIV → particle and fluid (seeded with fingerprint powder) velocities



Accelerated movie ($\times 15$) of PMMA spheres + Triton X-100 (with Rhodamine 6G) at $Q_f = 4.1 \cdot 10^{-6} \text{ m}^3 \text{ s}^{-1}$ and corresponding particle and fluid velocity profiles

Velocity and concentration profiles

particle (●), fluid (●) velocities, and volume fraction (+)
 Borosilicate (left) and PMMA with seeded fluid (right)

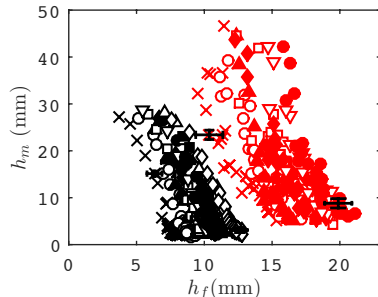
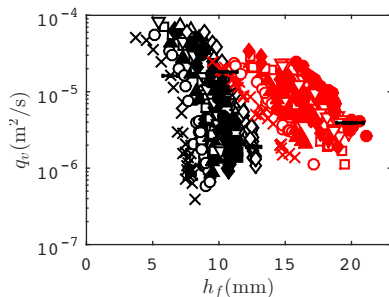


- **No velocity slip** between particles and fluid inside the mobile granular layer
- $\phi \approx \text{constant}$ inside the mobile granular layer except at the top interface where it vanishes on a distance $\approx 2d$

Particle-velocity flux q_v and mobile-layer thickness h_m

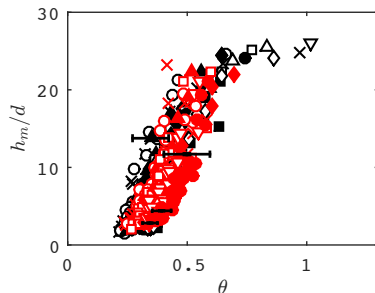
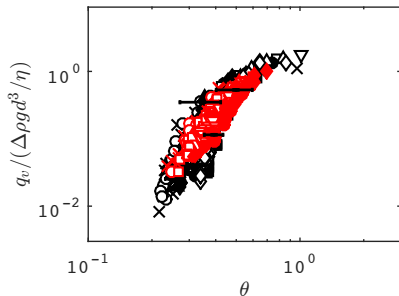
borosilicate: $Q_f = 2.7$ (×), 3.6 (○), 4.4 mm (▲), 5.3 (□), 5.7 (◆), 6.1 (▽), 6.9 (●), 8.2 (△), 8.6 (■), 9.7 cm³/s (◇)

PMMA: $Q_f = 2.2$ (×), 2.7 (○), 3.2 mm (▲), 3.6 (□), 4.1 (◆), 4.6 (▽), 5.6 cm³/s (●)



Decrease with increasing h_f but strong dependence on particle and fluid combination (**borosilicate** and **PMMA**) as well as fluid flow rate Q_f .

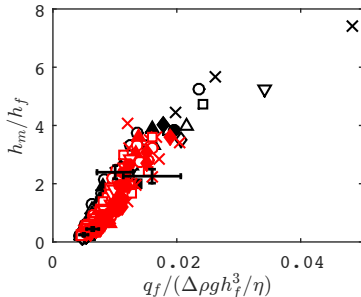
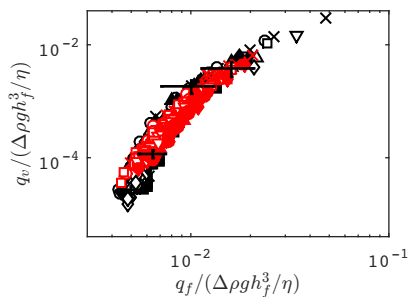
Scalings: length-scale = d and time-scale = $\eta/\Delta\rho gd$



Imperfect collapse of data

Shields number θ not the most appropriate parameter!

Scalings: length-scale = h_f and time-scale = $\eta/\Delta\rho gh_f$

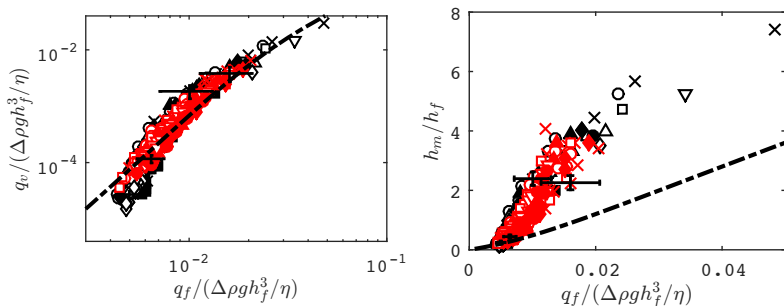


Good collapse using the scalings of the continuum two-phase approach

Control parameter = dimensionless fluid flow-rate $q_f / (\Delta\rho gh_f^3 / \eta)$

Comparison with Coulomb frictional rheology

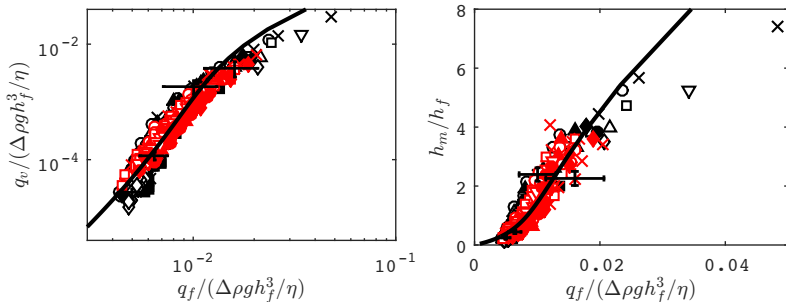
2D calculation with $\mu_s = 0.32$ and Einstein viscosity $\eta_e/\eta = 2.4$ (dashed line)



Realistic prediction for particle flux but not for bed-load thickness!

Comparison with Coulomb frictional rheology

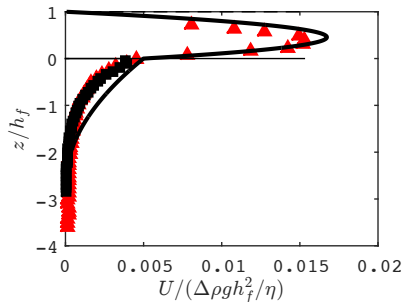
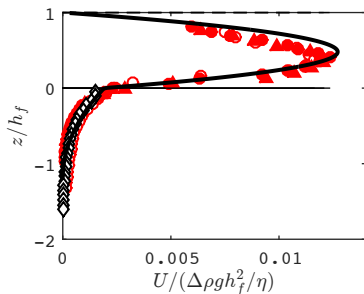
2D calculation with (best fit) $\mu_s = 0.24$ and $\eta_e/\eta = 14$ (solid line)



Good agreement except at large flow rate
but μ_s slightly low and η_e/η slightly high!

Velocity profiles versus Coulomb model

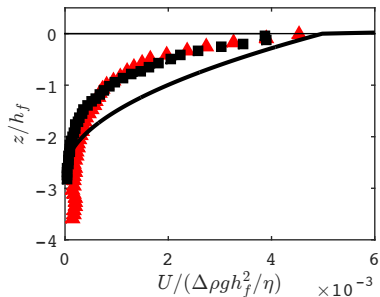
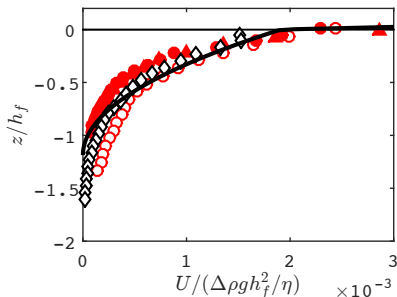
$q_f/(\Delta\rho gh_f^3/\eta) = 9.1 \cdot 10^{-3}$ (left) and $q_f/(\Delta\rho gh_f^3/\eta) = 13.9 \cdot 10^{-3}$ (right)



- Good collapse of the experimental data using the scalings of the continuum two-phase approach
- Good agreement between experimental data and 2D calculation with Coulomb frictional rheology in the pure fluid zone but not in the mobile layer zone!

Velocity profiles versus Coulomb model (blow-up)

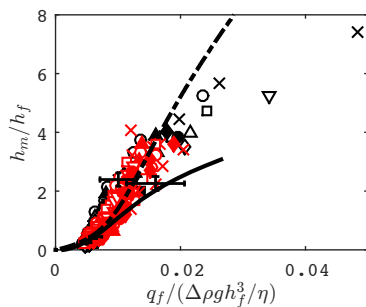
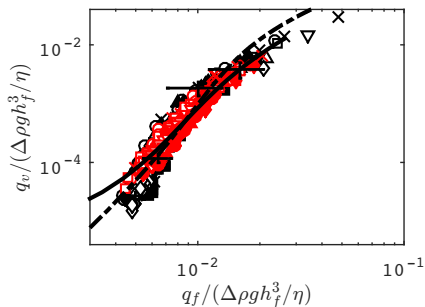
$q_f/(\Delta\rho gh_f^3/\eta) = 9.1 \cdot 10^{-3}$ (left) and $q_f/(\Delta\rho gh_f^3/\eta) = 13.9 \cdot 10^{-3}$ (right)



Velocity profile not well described by a simple parabola!

Comparison with granular frictional rheology $\mu(I_v)$

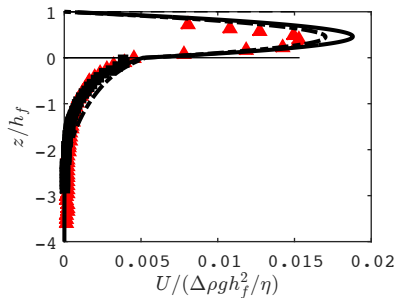
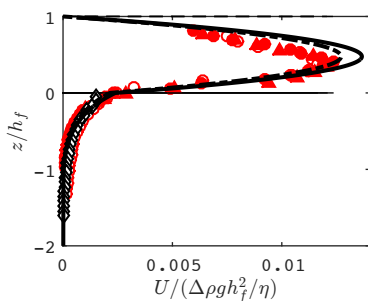
$\mu_s = 0.24$, $\mu_2 = 0.39$, $I_0 = 0.01$, and $\eta_e/\eta_f = 6.6$ (2D: dashed line and 3D: solid line)



- 2D model: good agreement but 3D effects at large flow rate
- 3D model: good agreement for q_v but underestimation for h_m at large flow rate

Velocity profiles versus granular model

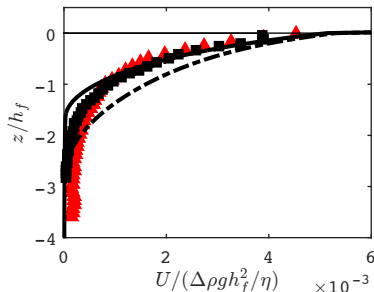
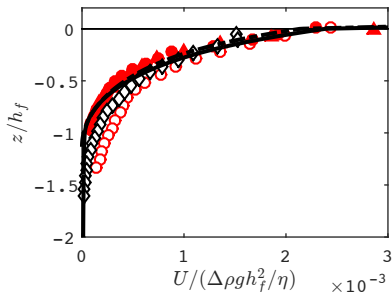
$q_f/(\Delta\rho gh_f^3/\eta) = 9.1 \cdot 10^{-3}$ (left) and $q_f/(\Delta\rho gh_f^3/\eta) = 13.9 \cdot 10^{-3}$ (right)



- Small flow rate: excellent agreement for 2D and 3D models
- Larger flow rate:
 - 2D model: good predictions in fluid / overestimation in bed-load
 - 3D model: good prediction in bed-load / overestimation in fluid

Velocity profiles versus granular model (blow-up)

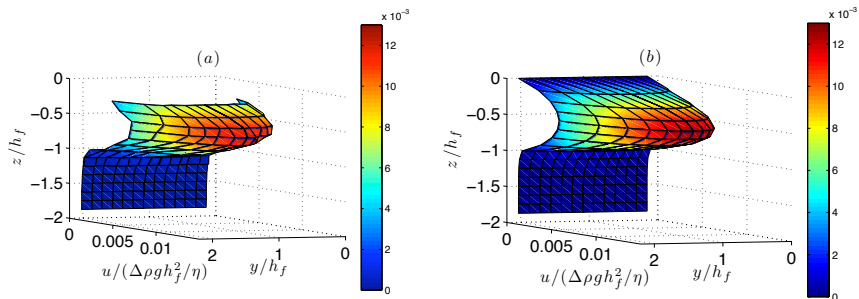
$q_f/(\Delta\rho gh_f^3/\eta) = 9.1 \cdot 10^{-3}$ (left) and $q_f/(\Delta\rho gh_f^3/\eta) = 13.9 \cdot 10^{-3}$ (right)



- Small flow rate: excellent agreement for 2D and 3D models
- Larger flow rate:
 - 2D model (dashed line): overestimation in bed-load
 - 3D model (solid line): good prediction in bed-load

Three-dimensional effects

(a) experimental and (b) numerical velocity profiles for PMMA at $Q_f = 4.1210^{-6} \text{ m}^3 \text{ s}^{-1}$ and $h_f = 16 \text{ mm}$



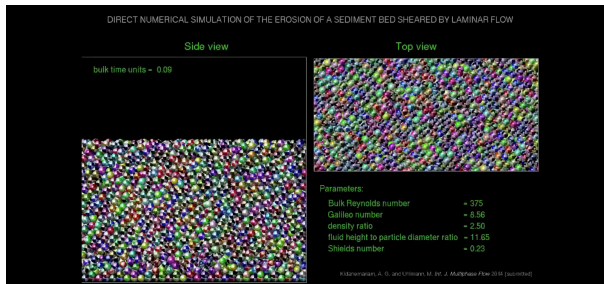
Good agreement

- 1 Incipient motion
- 2 Bed-load transport: a two-phase approach
- 3 Inside the bed-load
- 4 Bed-load transport: a discrete approach**
- 5 Dunes

Direct numerical simulation of the erosion of a sediment bed sheared by laminar channel flow

Immersed boundary technique for the fluid-solid coupling

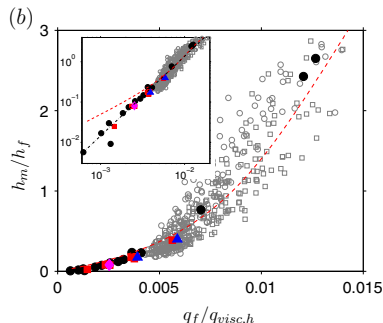
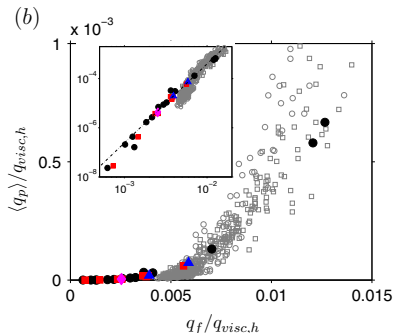
Soft-sphere approach for solid-solid contact



Kidanemariam and Uhlmann IJMF 2014

Comparison of experiments with discrete approach

Two-phase granular model (dashed red line)



Excellent agreement between experimental data of Aussillous, Chauchat, Pailha, Médale, and Guazzelli JFM 2013 and numerical simulation of Kidanemariam and Uhlmann IJMF 2014

- 1 Incipient motion
- 2 Bed-load transport: a two-phase approach
- 3 Inside the bed-load
- 4 Bed-load transport: a discrete approach
- 5 Dunes**

Bed evolution in a pipe

No motion



Flat bed in motion



Laminar dunes



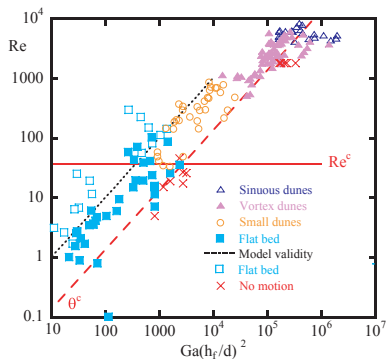
Vortex dunes



Sinuuous dunes



Phase diagram of the dune patterns



- Incipient motion:

$$Re \propto \theta^c Ga \left(\frac{h_f}{d} \right)^2$$

- Instability threshold:

$$Re^c \approx 37.5$$

(Galileo number = Re based on the Stokes velocity of the particles)

Ouriemi, Aussillous, and Guazzelli JFM 2009 Part 2

Nonlinear and turbulent ...

- Vortex dunes



Top view



Side view

- Sinuous dunes



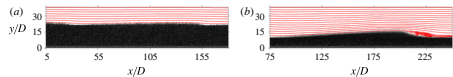
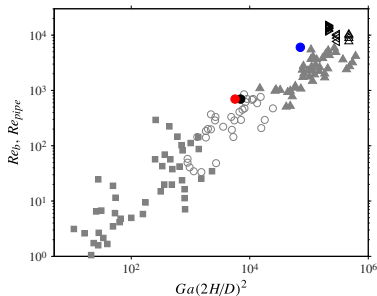
Top view



Side view

Dunes in direct numerical simulations

Kidanemariam and Uhlmann JFM 2014



(a) Small dunes (●) and (b) Vortex dunes (●)

Two cases in laminar flow (with different Galileo and Shields numbers) lead to the formation of 'small dunes', while one case under turbulent flow conditions exhibits 'vortex dunes', consistently with the regime classification of Ouriemi, Aussillous, and Guazzelli JFM 2009 Part 2

- 1 Incipient motion
- 2 Bed-load transport: a two-phase approach
- 3 Inside the bed-load
- 4 Bed-load transport: a discrete approach
- 5 Dunes

Conclusions

Understanding the erosion and transport by shearing flows of solid heavy particles forming an erodible bed:

- 1 Incipient motion: critical Shields number $\theta^c \approx 0.12$
independent of Reynolds number
- 2 Particle transport above this threshold:
 - Control parameter: dimensionless fluid flow-rate
 - Realistic predictions given by two-phase model using a frictional rheology as well as discrete simulations
- 3 Dunes:
 - Instability threshold: pipe Reynolds number
 - Regimes of 'small dunes', 'vortex dunes', and 'sinuous dunes'